METHOD FOR EVALUATING THE STRUCTURAL DYNAMICS INFLUENCE ON THE FLIGHT MECHANICS OF A FLEXIBLE AIRCRAFT

Flávio José Silvestre, flaviojs@ita.br
Pedro Paglione, paglione@ita.br
Instituto Tecnológico de Aeronáutica, Divisão de Engenharia Aeronáutica, Departamento de Mecânica do Vôo
Praça Marechal Eduardo Gomes, 50 - Vila das Acácias
CEP 12228-900 – São José dos Campos – SP – Brasil

Abstract. *In this paper, the equations of the three-dimensional flexible aircraft motion are stated using Lagrange's equations and the mean axes assumption. The incompressible quasi-steady strip theory aerodynamics approximation is used in modeling the incremental aerodynamic loads due to structural vibration, which dynamics is modeled through the modal decomposition technique. Doing so, the structural vibration influence on the aircraft flight mechanics is evaluated in terms of generalized structural stability derivatives. The flexible model is applied to a generic aircraft and the flight time responses are compared to the rigid body approximation. For checking the coherence of the developed computational routine, the generalized stability derivatives signals are then discussed.*

Keywords*: flexible aircraft, flight mechanics, aeroelasticity, strip theory*

NOMENCLATURE

AC	aerodynamic center
EA	elastic axis
CG	center of gravity
ARF	Aerodynamic Reference Frame
BRF	Body Reference Frame
X, Y, Z	forces on the BRF
$\underline{L}, \underline{M}, \underline{N}$	moments on the BRF
u, v, w	aircraft speed components on the BRF
p, q, r	aircraft angular speed components on the BRF
η_i	amplitude of the i-th vibration mode
ℓ	lift per unit span
d	drag per unit span
m_{AC}	moment around AC per unit span
$\mathbf{F}$ or $\vec{F}$	vector form
Φ_i	shape of the i-th vibration mode
Q	generalized force
C_{Ab}	influence coefficient of A due to b
$\mathbf{D}^*$	diagonal matrix with main diagonal $\begin{bmatrix}\bar{b} & \bar{c} & \bar{b}\end{bmatrix}$
$\mathbf{L}_{B/A}$	transformation matrix, from ARF to BRF
d_{EA}^{AC}	distance between AC and EA
x_{AC}	AC position for each span station, on the BRF
z^*	-z
δ_x	control surface deflection
τ_x	control surface "angle of attack" effectiveness

1 INTRODUCTION

DURING the last 40 years the number of research works about flight mechanics of flexible aircrafts has increased, mainly due to the design specifications of the new transport aircrafts. To reduce the aircraft empty weight the aeronautical industry low mass fraction structures, light materials and high stress design level. The demand to increase the aircraft capacity requires long fuselages, and in parallel the drag reduction for fuel saving orders for thin airfoils lifting surfaces and slender fuselages. Consequently the aircraft becomes large, very light and an increase of its structural flexibility can be observed [20].

The increase of the structural flexibility is accomplished by a reduction of the separation bandwidth between the rigid body and the structural vibration characteristic frequencies, what means that the influence of the structural dynamics on the aircraft flight mechanics can not be neglected. Then the classical approach which treats aeroelasticity [1] and the flight mechanics of a rigid body [13] independently must give place to an integrated model.

Besides, a new category of aircrafts is being nowadays developed, the so called UAV (Unmanned Air Vehicles), which are designed to carry out very critical maneuvers, well in excess of what pilots are able to tolerate [7]. The high load factor maneuvers cause structural deformation, which can be not negligible, demanding also an integrated approach which takes into account the interactions between flight mechanics and aeroelasticity.

This interaction is processed specially through the aerodynamic loading and the mass distribution. As the aircraft maneuvers, the aerodynamic loading changes and causes variations on the structural displacements in the volume, which alters the mass distribution and consequently the CG position and inertia dyadic, directly related to the maneuver characteristics. Also, the structural displacements modify directly the aerodynamic loading through the body geometrical transformation and due to motion. A schematic interaction representation can be found in Figure 1.1.

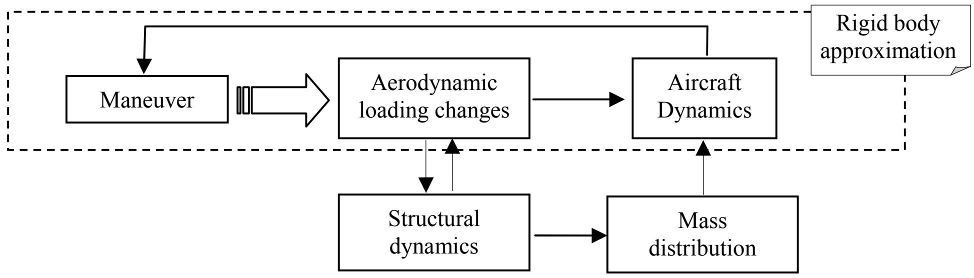

Figure 1.1- Integrated flight mechanics model interaction

Milne[12] was one of the pioneers on developing such a model. In [12] he makes use of the strip theory to represent the incremental aerodynamic loads and describes with a linear approach the aircraft three degrees of freedom motion (u, w, e θ), being the structural dynamics solved by imposition of the stress-strain relations and the displacements compatibility on control points. Also an important discussion about the axes choice for the equations statement is presented and the mean axes advantages in reducing the coupling between the rigid and elastic degrees of freedom become evident.

Adopting the mean axes, Cavin III and Dusto[4] apply the Lagrange's formulation and develop the general equations for the flexible aircraft. The same methodology is present in the works of Waszak et al.[18], [19] and Schimidt et al.[14], and an additional simplification is assumed, without demonstration, that the mean axes and the body reference frame fixed on the non-deformed aircraft can be assumed coincident, eliminating the inertial coupling between the rigid body variables and the elastic degrees of freedom. The structural dynamics is modeled through the modal decomposition technique and the strip theory is again invoked. The model developed and applied to the longitudinal motion is similar to the rigid body approximation and the structural dynamics influence is measured through generalized stability derivatives, similar to the classical treatment to the stability derivatives due to aircraft state[13]. A more precise model considering inertial coupling is presented by Butrtrill et. al.[3] and the main conclusions are that the inertial coupling becomes important when the aerodynamic loads are small or the angular rates are of the same magnitude that the vibration frequencies. A detailed comparison can be found in [17].

In [10] Meirovitch and Tuzcu points the disadvantages of choosing the mean axes due to the algebra manipulation on forces axes transformations and the variation on inertia dyadic. Without these transformations (simplification of Waszak et al.[18], [19]), the final result is considered questionable. Then in [8], [9] and [10], Meirovitch and Tuzcu apply the lagrangean formulation for developing the aircraft flight equations on a reference frame fixed on the non-deformed structure. The vibration influence is modeled as a part of low importance on the aircraft state. Then the equations generate two systems, one independent which is exactly the rigid body approximation, and that generates input on the other, the elastic effect part dynamics.

This paper is an extension of the work developed by Waszak et al.[18], [19] and Schimidt et al.[14]. The mean axes is assumed as the reference frame keeping the model simplicity and this assumption is further demonstrated to hold for a standard flight maneuver. The two-dimensional strip theory aerodynamics, under quasi-steady approach and incompressible flow is assumed to determine the incremental forces and moments due to the structural vibration, which model is based on the modal superposition technique. The generalized stability derivatives for the complete three-dimensional flight are analytically and numerically evaluated and a further discussion about its signals based on physical considerations is performed. The same aircraft described in [18] is used, as well as its two first vibration modes, one symmetric and another anti-symmetric. Time response simulations and poles mapping help to compare the flexible aircraft behavior and the rigid body approach.

2 MODAL SUPERPOSITION

Following the methodology presented by Bismarck [1], approximating the structure of the aircraft of a linear discrete system with n degrees of freedom, the application of an external load places the point P_0 on the new position P, so we can write, in terms of the generalized coordinates:

$$\mathbf{P} = \left[\frac{\partial \mathbf{P}}{\partial q_1} \; \frac{\partial \mathbf{P}}{\partial q_2} \cdots \frac{\partial \mathbf{P}}{\partial q_n} \right] \begin{Bmatrix} q_1 \\ q_2 \\ \vdots \\ q_n \end{Bmatrix} = \frac{\partial \mathbf{P}}{\partial q_i} q_i = \mathbf{N}\{q\} \tag{2.1}$$

Then, the kinetic and strain energy expressions can be derived, as follows:

$$T=\frac{1}{2}\int_V \rho(\mathbf{P})\mathbf{V}(\mathbf{P}).\mathbf{V}(\mathbf{P})\,dV=\frac{1}{2}\{q'\}^T\mathbf{M}\{q'\} \quad \Big| \quad U_S=\frac{1}{2}\int_V \boldsymbol{\sigma}^T\{\boldsymbol{\varepsilon}\}\,dV=\frac{1}{2}\{q\}^T\mathbf{K}\{q\} \tag{2.2}$$

where **M** and **K** are, respectively, the mass and stiffness matrices associated to the system, and are symmetrical positive-definite matrices.

Assuming that the damping forces in the system are of a viscous nature and depend linearly on the speed of each point mass, the dissipation force of the system as well as the dissipation energy (from the Principle of Virtual Work) can be then evaluated, as follows.

$$\mathbf{F}_D(\mathbf{P})=\frac{\partial \mathbf{F}_D(\mathbf{P})}{\partial q_i'}q_i' \Rightarrow \Gamma=\frac{W_D}{\Delta t}=\frac{1}{2}\{q'\}^T\mathbf{B}\{q'\} \tag{2.3}$$

where **B** is the dissipation matrix.

Applying the Langrage's Equations derived from the Extended Hamilton's Principle [11] to the system, one can obtain the equations of structural motion:

$$\frac{d}{dt}\left(\frac{\partial L}{\partial q_i'}\right)-\frac{\partial L}{\partial q_i}+\frac{\partial \Gamma}{\partial q_i'}=Q_i \Rightarrow \mathbf{M}\{q''\}+\mathbf{B}\{q'\}+\mathbf{K}\{q\}=\{F\} \tag{2.4}$$

where $L=T-U_S$ and $\{F\}$ are the external applied loads.

Assuming that $\{q\}=\{q_0\}e^{P_i\times t}$ and $\lambda_i=-P_i^2$, the free undamped problem leads the eigenvalue problem below:

$$\left(\mathbf{K}-\lambda_i\mathbf{M}\right)\{q_0\}=\{0\} \tag{2.5}$$

The modal superposition technique consists in writing the generalized coordinates of the structural equations of motion in the base formed by the eigenvectors **Q** of problem (2.5) through modal amplitudes $\{\eta\}$. Then substituting into equation (2.4) and pre-multiplying by $\mathbf{Q}^T$ one has:

$$\{q\}=\mathbf{Q}\{\eta\} \overset{\text{Eq.(2.6)}}{\Rightarrow} \boldsymbol{\mu}\{\eta''\}+\boldsymbol{\beta}\{\eta'\}+\boldsymbol{\gamma}\{\eta\}=\{\varphi\} \tag{2.6}$$

where **μ**, **β** and **γ** are the generalized mass, damping and stiffness matrices. Due to the eigenvectors orthogonality, **μ** and **γ** are diagonal, and **β** can be supposed approximately diagonal [10]. Then equation (2.6) becomes, simply:

$$\boldsymbol{\mu}_{ii}\,\eta_i''+\boldsymbol{\beta}_{ii}\,\eta_i'+\boldsymbol{\gamma}_{ii}\,\eta_i=\varphi_i \Leftrightarrow \eta_i''+2\xi_i\omega_{n,i}\;\eta_i'+\omega_{n,i}{}^2\;\eta_i=\frac{\varphi_i}{\boldsymbol{\mu}_{ii}},\quad i=1,2,...,n \tag{2.7}$$

where ξ_i and $\omega_{n,i}$ are the modal damping and natural frequency. Observe that, using the modal basis, the expressions of kinetic, strain and dissipation energies can also be simplified. Then:

$$\mathbf{P}=\mathbf{N}\{q\}=\mathbf{NQ}\{\eta\}=\boldsymbol{\Phi}(x,y,z)\{\eta\} \tag{2.8}$$

where $\boldsymbol{\Phi}(x,y,z)$ are the mode shapes, which can be obtained through a finite element analysis for a complex structure.

3 EQUATIONS OF MOTION

Consider now a flying airplane and its reference frames as in Figure 3.1. Again Lagrange's equations will be applied for the deduction of the equations of motion, repeating intentionally, for remembrance, the same methodology as in [19]. The kinetic energy expression can be evaluated as follows:

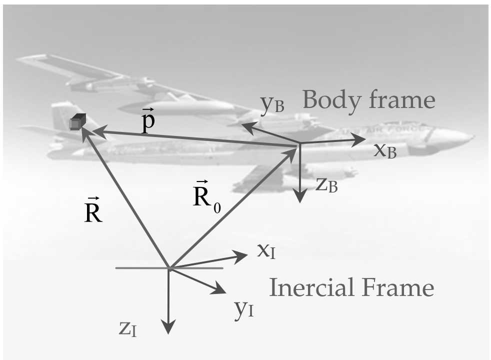

Figure 3.1- Flying aircraft and its reference frames

$$T=\frac{1}{2}\int_V \frac{d\vec{R}}{dt}\cdot\frac{d\vec{R}}{dt}\rho dV=\frac{1}{2}\int_V\left(\frac{d\vec{R}_0}{dt}+\frac{d\vec{p}}{dt}\right)\cdot\left(\frac{d\vec{R}_0}{dt}+\frac{d\vec{p}}{dt}\right)\rho dV \tag{3.1}$$

$$\begin{cases}\dfrac{d\vec{R}_0}{dt}=\left.\dfrac{d\vec{R}_0}{dt}\right|_B+\vec{\omega}\times\vec{R}_0\triangleq u\vec{i}_B+v\vec{j}_B+w\vec{k}_B\\ \vec{R}_0=x\vec{i}_B+y\vec{j}_B+z\vec{k}_B\\ \vec{\omega}=p\vec{i}_B+q\vec{j}_B+r\vec{k}_B\\ \dfrac{d\vec{p}}{dt}=\left.\dfrac{d\vec{p}}{dt}\right|_B+\vec{\omega}\times\vec{p}\end{cases} \tag{3.2}$$

Note that the derivative $\left.\frac{d\vec{p}}{dt}\right|_B$ is due to the structural dynamics, which was discussed in 3. Adopting the mean axes as the reference body frame, located at the instantaneous aircraft CG [19], and assuming that for small displacements the mean axes can be considered coincident to the body reference frame fixed on the CG of the undeformed aircraft, then the structural dynamics influence can be decoupled:

$$T=\frac{1}{2}m\frac{d\vec{R}_0}{dt}\cdot\frac{d\vec{R}_0}{dt}+\frac{1}{2}\{\omega\}^T\mathbf{I}\{\omega\}+\frac{1}{2}\sum_{i=1}^{n}\mu_{ii}\left(\eta_i'\right)^2 \tag{3.3}$$

where **I** is the aircraft inertia dyadic, supposed constant for small deformations. For small displacements, the mean axes remains very close to the body reference frame, and can be so approximated for it. The kinematics and geometrical transformations [13] make the kinetic energy to be a function of the aircraft position coordinates (written on the body reference frame), the Euler angles, the modal amplitudes, and their rates. The gravitational potential energy and the strain energy compose the system's potential energy:

$$\begin{aligned}&U_G=-\frac{1}{2}\int_V\vec{R}\cdot\vec{g}\rho dV=-mg\left(\mathbf{L}_{I/B}(3,:)\begin{bmatrix}x & y & z\end{bmatrix}^T\right)\\ &U_S=\frac{1}{2}\int_V\boldsymbol{\sigma}^T\{\boldsymbol{\varepsilon}\}dV=\frac{1}{2}\{q\}^T\mathbf{K}\{q\}=\frac{1}{2}\sum_{i=1}^{n}\mu_{ii}\omega_{n,i}{}^2\eta_i{}^2\\ &U=U_G+U_S\end{aligned} \tag{3.4}$$

where $\mathbf{L}_{I/B}$ is the transformation matrix from the body reference frame to the inertial one. Finally the dissipation energy:

$$\Gamma=\frac{W_D}{\Delta t}=\frac{1}{2}\{q'\}^T\mathbf{B}\{q'\}=\frac{1}{2}\sum_{i=1}^{n}\mu_{ii}\left(2\xi_i\omega_{n,i}\right)\left(\eta_i'\right)^2 \tag{3.5}$$

The generalized forces can be obtained through (3.6) [6]:

$$Q_k=\int_V\vec{f}\cdot\frac{\partial\vec{R}}{\partial q_k}dV \tag{3.6}$$

where $\vec{f}$ is the force per unit volume, which is not derived from a potential, it is, the aerodynamic forces. Then, $Q_x = X$, $Q_\phi = -Yz_{CG} + Zy_{CG} + \underline{L}$ and so on. Applying (2.4), together to geometrical transformations and kinematical relations, after some algebraic manipulation one comes up with the equations of motion of the elastic aircraft in terms of the linear and angular velocities' rate, and the second derivative of the modal amplitudes, as summarized by Waszak and Schmidt [19] and repeated here for convenience:

$$\begin{aligned}
&\dot{u} = \frac{X}{m} + rv - qw - g\sin\theta \\
&\dot{v} = \frac{Y}{m} - ru + pw + g\cos\theta\sin\phi \\
&\dot{w} = \frac{Z}{m} + qu - pv + g\cos\theta\cos\phi \\
&I_{xx}\dot{p} - I_{xy}\dot{q} - I_{xz}\dot{r} - I_{yz}\left(q^2 - r^2\right) - \left(I_{yy} - I_{zz}\right)qr - p\left(I_{xz}q - I_{xy}r\right) = \underline{L} \\
&-I_{xy}\dot{p} + I_{yy}\dot{q} - I_{yz}\dot{r} - I_{xz}\left(r^2 - p^2\right) - \left(I_{zz} - I_{xx}\right)pr - q\left(I_{xy}r - I_{yz}p\right) = \underline{M} \\
&-I_{xz}\dot{p} - I_{yz}\dot{q} + I_{zz}\dot{r} - I_{xy}\left(p^2 - q^2\right) - \left(I_{xx} - I_{yy}\right)pq - r\left(I_{yz}p - I_{xz}q\right) = \underline{N} \\
&\eta_i'' + 2\xi_i\omega_{n,i}\,\eta_i' + \omega_{n,i}^{\;2}\,\eta_i = Q_{\eta_i}/\boldsymbol{\mu}_{ii}\,, \quad i = 1,2,...,n
\end{aligned} \tag{3.7}$$

4 INCREMENTAL AERODYNAMICS MODEL

The determination of the incremental aerodynamic loads and moments is made through the strip theory [5], which considers that, for any lifting surface, the chordwise pressure distribution at any spanwise station depends only on the downwash at that station as in the two-dimensional aerodynamic theory, and is independent of the downwash of any other spanwise station. Under the quasi-steady incremental aerodynamics, the airfoil movement history influence is neglected (no delay between the airfoil movement and the aerodynamic resultant generation). The forces per unit span at each section are considered to be generated at the quarter-chord, and the equivalent torsion and displacement are evaluated at the elastic axes, linearizing the modal shape function at that axes.

The lifting surfaces bend and torsion are taken into account only in terms of effective attack angle and side slip angle, but one considers that the surface deformation does not modify the profile capacity of generating lift.

Then, the variation on the effective sideslip and attack angles at each section of the considered lifting surface can be expressed as:

$$\Delta\alpha_s = \sum_{i=1}^{n}\left(\underbrace{\frac{1}{u}\Phi_i^{\,e}\eta_i'}_{\text{bending}} - \underbrace{\frac{d\Phi_i^{\,e}}{dx}\eta_i}_{\text{torsion}}\right) \qquad \Bigg| \qquad \Delta\beta_s = \sum_{i=1}^{n}\left(\underbrace{\frac{1}{u}\Phi_i^{\,e}\eta_i'}_{\text{bending}} - \underbrace{\frac{d\Phi_i^{\,e}}{dx}\eta_i}_{\text{torsion}}\right) \tag{4.1}$$

Consequently, variations on the aerodynamic forces and moments due to deformations of wings, horizontal and vertical empennages are expected. The fuselage's contributions will be neglected. Let us firstly work with the wing and the horizontal empennage. Considerer, for each section of the lifting surface, the variation on the lift and drag for unit span:

$$\Delta\ell = \frac{1}{2}\rho V^2 c C_{\ell\alpha}\Delta\alpha_s \qquad \Bigg| \qquad \Delta d = \frac{1}{2}\rho V^2 c C_{d\alpha}\Delta\alpha_s \tag{4.2}$$

Then, integrating along the quarter-chord line and using the aerodynamic axes to body axes transformation matrix, we have (the subscript '*W, HE*' means wing and horizontal empennage contribution):

$$\begin{bmatrix}\Delta X\\ \Delta Y\\ \Delta Z\end{bmatrix}_{W,HE} = \int_{-b/2}^{b/2}\mathbf{L}_{B/A}\begin{bmatrix}-\Delta d(y)\\ 0\\ -\Delta\ell(y)\end{bmatrix}dy = \frac{1}{2}\rho V^2 S\left(-\frac{1}{S}\mathbf{L}_{B/A}\int_{-b/2}^{b/2}\begin{bmatrix}c(y)C_{d\alpha}(y)\Delta\alpha(y)\\ 0\\ c(y)C_{\ell\alpha}(y)\Delta\alpha(y)\end{bmatrix}dy\right) \tag{4.3}$$

For each i^{th} mode: $\begin{bmatrix}\Delta X_i\\ \Delta Y_i\\ \Delta Z_i\end{bmatrix}_{W,HE} = \frac{1}{2}\rho V^2 S\left(\frac{1}{S}\mathbf{L}_{B/A}\int_{-b/2}^{b/2} c(y)\begin{bmatrix}C_{d\alpha}(y)\\ 0\\ C_{\ell\alpha}(y)\end{bmatrix}\frac{\partial \Phi_{z,i}{}^{e}}{\partial x}(y)\,dy\right)\eta_i +$

$$+\frac{1}{2}\rho V^2 S\frac{\mathbf{D}^*}{2V_e}\left(-\left(2V_e(\mathbf{D}^*)^{-1}\right)\frac{1}{Su}\mathbf{L}_{B/A}\int_{-b/2}^{b/2} c(y)\begin{bmatrix}C_{d\alpha}(y)\\ 0\\ C_{\ell\alpha}(y)\end{bmatrix}\Phi_{z,i}{}^{e}(y)\,dy\right)\eta_i' = \tag{4.4}$$

$$=\frac{1}{2}\rho V^2 S\left(\begin{bmatrix}C_{X\eta_i}\\ C_{Y\eta_i}\\ C_{Z\eta_i}\end{bmatrix}_{A,EH}\eta_i + \frac{\mathbf{D}^*}{2V_e}\begin{bmatrix}C_{X\eta'_i}\\ C_{Y\eta'_i}\\ C_{Z\eta'_i}\end{bmatrix}_{A,EH}\eta_i'\right)$$

where $\mathbf{D}^*$ is the normalization diagonal matrix with diagonal $\left(\bar{c}\quad b\quad \bar{c}\right)$. If $\vec{r}$ is the position of the quarter-chord at any station, written on the body reference frame, then the generated moments due to the structural dynamics can be evaluated as:

$$\begin{bmatrix}\Delta \underline{L}\\ \Delta \underline{M}\\ \Delta \underline{N}\end{bmatrix}_{W,HE} = \int_{-b/2}^{b/2}\vec{r}(y)\times\left(\mathbf{L}_{B/A}\begin{bmatrix}-\Delta d(y)\\ 0\\ -\Delta\ell(y)\end{bmatrix}\right)dy = \frac{1}{2}\rho V^2 S\mathbf{D}^{**}\left(-\frac{(\mathbf{D}^{**})^{-1}}{S}\int_{-b/2}^{b/2}\vec{r}(y)\times\left(\mathbf{L}_{B/A}\begin{bmatrix}c(y)C_{d\alpha}(y)\Delta\alpha(y)\\ 0\\ c(y)C_{\ell\alpha}(y)\Delta\alpha(y)\end{bmatrix}\right)dy\right) \tag{4.5}$$

For each i^{th} mode: $\begin{bmatrix}\Delta \underline{L}_i\\ \Delta \underline{M}_i\\ \Delta \underline{N}_i\end{bmatrix}_{W,HE} = \frac{1}{2}\rho V^2 S\mathbf{D}^{**}\left(\frac{(\mathbf{D}^{**})^{-1}}{S}\int_{-b/2}^{b/2}\vec{r}(y)\times\left(\mathbf{L}_{B/A}c(y)\begin{bmatrix}C_{d\alpha}(y)\\ 0\\ C_{\ell\alpha}(y)\end{bmatrix}\frac{\partial \Phi_{z,i}{}^{e}}{\partial x}(y)\right)dy\right)\eta_i +$

$$+\frac{1}{2}\rho V^2 S\mathbf{D}^{**}\frac{\mathbf{D}^{**}}{2V_e}\left(-2V_e((\mathbf{D}^{**})^2)^{-1}\frac{1}{Su}\int_{-b/2}^{b/2}\vec{r}(y)\times\left(\mathbf{L}_{B/A}c(y)\begin{bmatrix}C_{d\alpha}(y)\\ 0\\ C_{\ell\alpha}(y)\end{bmatrix}\Phi_{z,i}{}^{e}(y)\right)dy\right)\eta_i' \tag{4.6}$$

$$=\frac{1}{2}\rho V^2 S\mathbf{D}^{**}\left(\begin{bmatrix}C_{\underline{L}\eta_i}\\ C_{\underline{M}\eta_i}\\ C_{\underline{N}\eta_i}\end{bmatrix}_{A,EH}\eta_i + \frac{\mathbf{D}^{**}}{2V_e}\begin{bmatrix}C_{\underline{L}\eta'_i}\\ C_{\underline{M}\eta'_i}\\ C_{\underline{N}\eta'_i}\end{bmatrix}_{A,EH}\eta_i'\right)$$

where $\mathbf{D}^{**}$ is the normalization diagonal matrix $diag\left(\bar{b}\quad \bar{c}\quad \bar{b}\right)$. The generalized forces acting on the modal amplitudes degrees of freedom can have a similar treatment in terms of influence coefficients. According to equation (3.6):

$$\underset{W,HE}{Q_{\eta_i}} = \int_V\left(f_z\Phi_i^e + f_z\left(x-x^e\right)\frac{\partial\Phi_i^e}{\partial x}\right)dV =$$
$$= \int_{-b/2}^{b/2}\left[L_{B/A}(3,:)\left[-d\quad 0\quad -\ell\right]^T\Phi_i^e - m_{CA}\frac{\partial\Phi_i^e}{\partial x} + L_{B/A}(3,:)\left[-d\quad 0\quad -\ell\right]^T\left(x_{CA}-x^e\right)\frac{\partial\Phi_i^e}{\partial x}\right]dy \tag{4.7}$$

Considering now that the local angle of attack at each section of the wing and the horizontal empennage as:

$$\alpha_s = \alpha + i_s - \frac{qx_{CA}}{u} + \frac{py}{u} + \Delta\alpha_s \tag{4.8}$$

expression (4.7) can be put into the form:

$$\underset{W,HE}{Q_{\eta_i}} = \frac{1}{2}\rho V^2 S\bar{c}\left\{C_{\eta_i,0} + C_{\eta_i,\alpha}\alpha + \sum_{k=1}^{n}C_{\eta_i,\eta_k} + \frac{\bar{c}}{2V_e}\left(C_{\eta_i,p}p + C_{\eta_i,q}q + \sum_{k=1}^{n}C_{\eta_i,\dot{\eta}_k}\dot{\eta}_k\right)\right\} \tag{4.9}$$

$$C_{\eta_i,0} = \frac{1}{S\bar{c}} \int_{-b/2}^{b/2} c \left\{ -\left(\Phi_i^e + \left(x_{CA} - x^e \right) \frac{\partial \Phi_i^e}{\partial x} \right) L_{B/A}(3,:) \begin{bmatrix} C_{d0} + C_{d\alpha} i_s \\ 0 \\ C_{\ell 0} + C_{\ell\alpha} i_s \end{bmatrix} - \frac{\partial \Phi_i^e}{\partial x} \bar{c}\, c_{m_{CA}} \right\} dy \quad (4.10)$$

$$C_{\eta_i,\alpha} = \frac{1}{S\bar{c}} \int_{-b/2}^{b/2} c \left\{ -\left(\Phi_i^e + \left(x_{CA} - x^e \right) \frac{\partial \Phi_i^e}{\partial x} \right) L_{B/A}(3,:) \begin{bmatrix} C_{d\alpha} \\ 0 \\ C_{\ell\alpha} \end{bmatrix} \right\} dy \quad (4.11)$$

and so on for the other coefficients. Now, considering the vertical empennage, exactly the same approach is followed. Equations from (4.3) to (4.11) must be rewritten, changing the attack angle at each section by the sideslip angle, and, naturally, changing the aerodynamic force for unit span vector as well as the displacement and torsion vectors.

$$\beta_s = \beta + \frac{r\, x_{CA}}{u} - \frac{p\, z}{u} + \Delta\beta_s \quad (4.12)$$

Then, the vertical empennage contribution to the influence coefficients can be achieved. Equations (4.13) and (4.14) give, as an example of similarity, the expressions for the force coefficients and generalized force dependence with sideslip.

$$\begin{bmatrix} C_{X\eta_i} \\ C_{Y\eta_i} \\ C_{Z\eta_i} \end{bmatrix}_{VE} = \frac{1}{S} \mathbf{L}_{B/A} \int_0^{b/2} c(\hat{z}) \begin{bmatrix} C_{d\alpha}(\hat{z}) \\ C_{\ell\alpha}(\hat{z}) \\ 0 \end{bmatrix} \frac{\partial \Phi_{y,i}^e}{\partial x}(\hat{z})\, d\hat{z} \quad (4.13)$$

$$C_{\eta_i,\beta} = \frac{1}{S\bar{c}} \int_0^{b/2} c \left\{ -\left(\Phi_i^e + \left(x_{CA} - x^e \right) \frac{\partial \Phi_i^e}{\partial x} \right) L_{B/A}(2,:) \begin{bmatrix} C_{d\beta} \\ C_{\ell\beta} \\ 0 \end{bmatrix} \right\} d\hat{z} \quad (4.14)$$

5 STRUCTURAL DYNAMICS MODEL – MODAL SHAPES

The same two vibration modes (one symmetric and another anti-symmetric) obtained by Wazsak at all [18] were chosen to analyze the structural dynamics influence on the flight mechanics of the aircraft. Just the vertical displacement was considered for the wing and horizontal empennage, and the lateral displacement for the vertical empennage.

For working with the modal shape data, two kinds of interpolation polynomial surfaces, I1 and I2, were studied, summarized in Table 5.1:

Table 5.1- Interpolation types studied

(*) For the vertical empennage, $\Phi = \Phi(x,z)$

Interpolation	Expression	Number of Coefficients
I1	$\Phi(x,y) = \sum_{i=0}^{n} \sum_{j=0}^{n} a_{ij} x^i y^j ,\ i+j \le n$ (*)	$\frac{(n+1)(n+2)}{2}$
I2	$\Phi(x,y) = \sum_{i=0}^{n} [b_i(x)] y^i ,\ b_i(x) = \sum_{j=0}^{m} a_{ij} x^j$ (*)	$(m+1)(n+1)$

Both sets of coefficients were found fitting the modal shape data best in a least-square sense. Analyzing I1 and I2, for both vibration modes and for all the surfaces, it is notable the better capacity of I2 in fitting the data points, especially on the regions where the modal shape derivatives are greater. Interpolation errors lower than 2.5% of the mean aerodynamic chord were registered. In Figure 6.1 one can find the modal shapes considered and interpolated.

6 RESULTS

Table 6.1 summarizes all the generalizes stability and control derivatives for the flexible aircraft, where the green part corresponds to the calculated ones through the methodology herein presented.

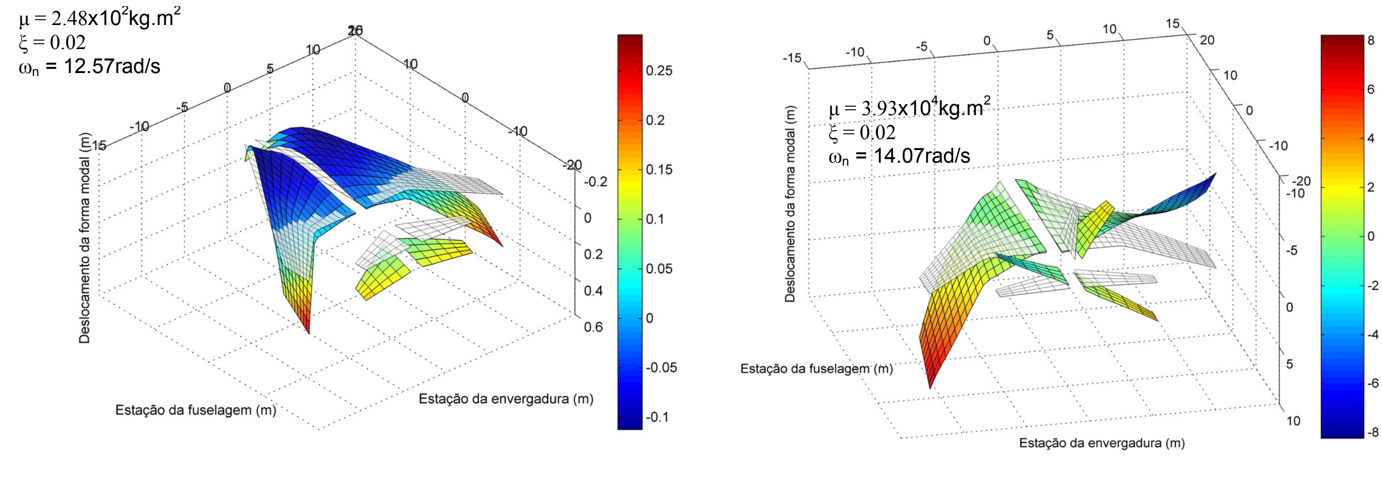

Figure 6.1- Undeformed aircraft and its symmetric and anti-symmetric mode shapes

Table 6.1- Generalized stability and control derivatives for the flexible aircraft

State	C_0	C_α	C_β	$C_{\dot\alpha}$	C_p	C_q	C_r	$C_{\delta a}$	$C_{\delta p}$	$C_{\delta r}$	C_{η_1}	$C_{\dot\eta_1}$	C_{η_2}	$C_{\dot\eta_2}$
C_X	-0.0280	0.2000	0.0000	0.0000	0.0000	-1.7000	0.0000	0.0000	0.2406	0.0000	-0.0014	0.0034	0.0000	0.0000
C_Y	0.0000	0.0000	-0.6300	0.0000	0.0000	0.0000	0.0000	-0.0286	0.0000	0.2406	0.0000	0.0000	-0.0259	-0.0771
C_Z	-0.3400	-2.9200	0.0000	0.0000	0.0000	14.7000	0.0000	0.0000	-0.4469	0.0000	-0.0262	-0.0451	0.0000	0.0000
C_L	0.0000	0.0000	-0.0570	0.0000	-0.0770	0.0000	0.1500	-0.0160	0.0000	0.0103	0.0000	0.0000	0.0954	0.0241
C_M	-0.2520	-1.6600	0.0000	-4.3000	0.0000	-34.7500	0.0000	0.0000	-2.4064	0.0000	-0.0664	-0.2632	0.0000	0.0000
C_N	0.0000	0.0000	0.1150	0.0000	-0.0800	0.0000	-0.1350	0.0069	0.0000	-0.0424	0.0000	0.0000	-0.0048	0.0270
$C_{Q\eta_1}$	0.0016	-0.0202	0.0000	0.0000	0.0000	-0.2059	0.0000	0.0000	-0.0128	0.0000	-0.0005	-0.0023	0.0000	0.0000
$C_{Q\eta_2}$	0.0000	0.0000	-0.1822	0.0000	0.1912	0.0000	0.8715	-0.3667	-0.0642	0.2733	0.0000	0.0000	-0.1797	-0.9524

*angles in [rad] and rates in [rad/s]; forces in [N] and moments in [N.m]

Based on the poles mapping presented in Figure 6.2 one can observe that the flexibility influence is greater on the short period and the dutch-roll modes. In the first, a frequency reduction is verified; in the second, an instable mode, an increase of the amplitudes amplification is noted. Those behaviors can be easily observed in the time responses due to excitations for both modes, showed in Figure 6.3.

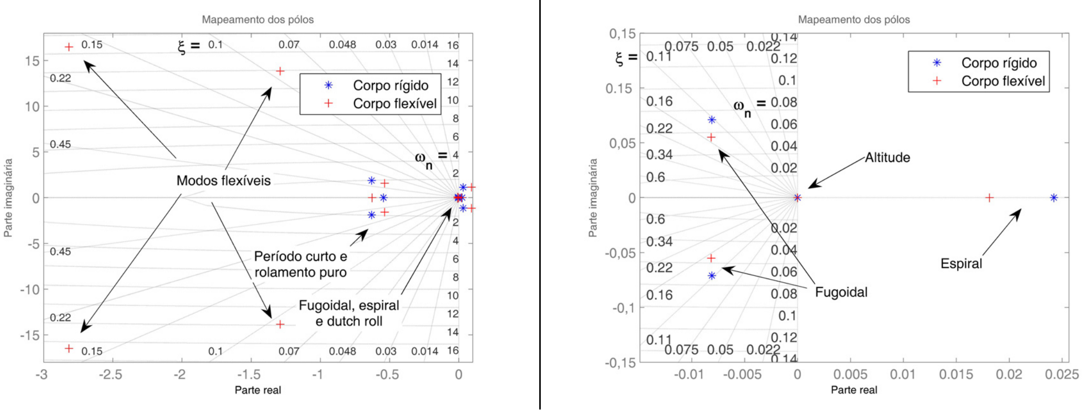

Figure 6.2- Poles mapping comparison between the flexible model and the rigid body approach

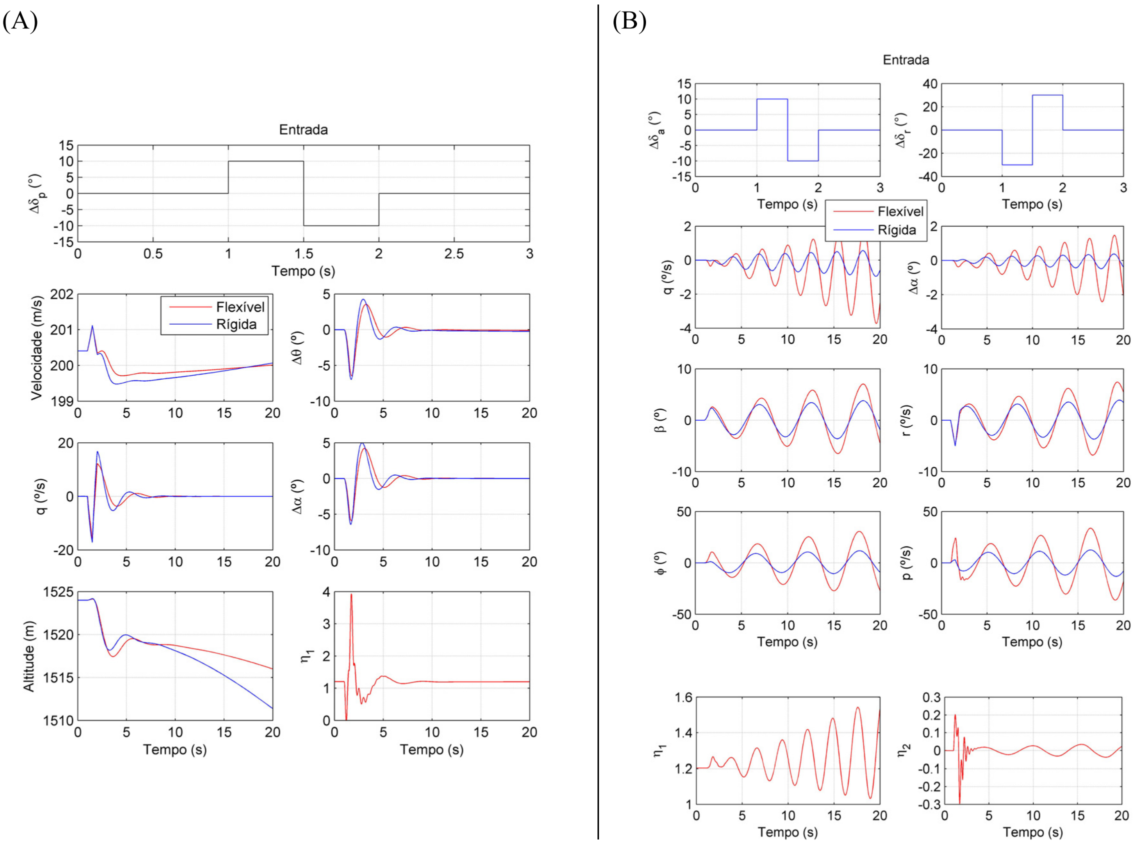

Figure 6.3- Time responses comparison for commanded motion: (A) short-period and (B) dutch-roll

For the evaluation of the generalized stability derivatives signals based on physical considerations, one should separate the influence of bending and torsion of the lifting surface. Then two fictitious mode shapes were generated for this purpose, as showed in Figure 6.4.

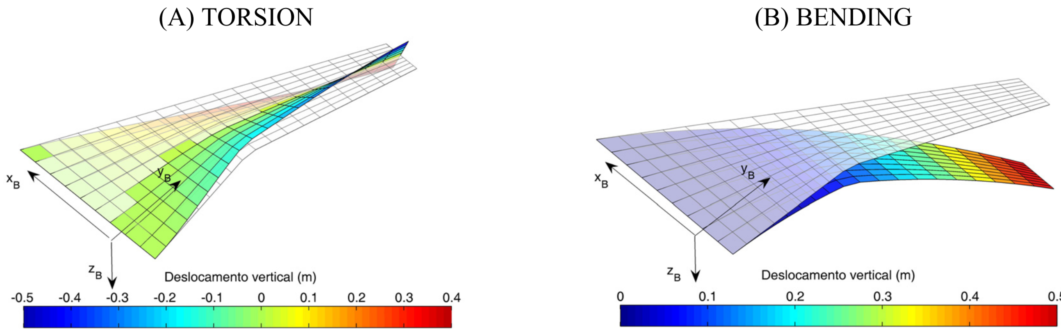

Figure 6.4- Fictitious mode shapes

For η_A positive, then a reduction of the angle of attack at each span section will generate a decrease in both lift and drag for unit span. In this case, according to the reference frame in the figure, it is easy to see that $C_{X\eta A} > 0$ and $C_{Z\eta A} > 0$. The right wing lift reduction causes positive rolling moment, so $C_{L\eta A} > 0$, and drag reduction causes a negative yaw moment, then $C_{N\eta A} < 0$. In addition, the great portion of the wing has the aerodynamic center behind the CG, so reduction in the lift reduce the pitch-down moment, and so $C_{M\eta A} > 0$.For η'_B positive, then an increase of the angle of attack at each span section will generate an increase in both lift and drag for unit span. In this case, based on the discussion above, $C_{X\eta A} < 0$, $C_{Z\eta A} < 0$. $C_{L\eta A} < 0$, $C_{N\eta A} > 0$ and $C_{M\eta A} < 0$.Now focusing on the generalized forces, note that increases on α, p and q induce a torsion opposite to (A) and a bending motion opposite to (B), and so: $C_{\eta,\alpha}$, $C_{\eta,p}$ and $C_{\eta,q}$ are negatives for both (A) and (B). In addition, increasing η_A the decrease on lift is in favor of the increase on η_A, so $C_{\eta A,\, \eta A} > 0$. An the increase on lift generate for the increase on η_B induce an opposite wing bending, so $C_{\eta B,\ \eta B} < 0$. Table 6.2 shows the method output for both mode shapes, in accordance with the previous discussion.

Table 6.2- Generalized stability derivatives for the fictitious mode shapes

$C_{X\eta A}$	$C_{Z\eta A}$	$C_{L\eta A}$	$C_{M\eta A}$	$C_{N\eta A}$	$C_{\eta A,\alpha}$	$C_{\eta A,p}$	$C_{\eta A,q}$	$C_{\eta A,\ \eta A}$
0.0029	0.0357	0.0129	0.0201	-0.0010	-0.0147	-0.0447	-0.0041	0.0013
$C_{X\eta B}$	$C_{Z\eta B}$	$C_{L\eta B}$	$C_{M\eta B}$	$C_{N\eta B}$	$C_{\eta B,\alpha}$	$C_{\eta B,p}$	$C_{\eta B,q}$	$C_{\eta B,\ \eta B}$
-0.0030	-0.0389	-0.0028	-0.0214	0.0002	-0.0194	-0.0672	-0.0214	-0.0024

Finally, for the confirmation of the hypothesis that the mean axes during the flight is so near to the body reference frame fixed on the CG of the non-deformed aircraft that both reference frames can be considered coincident, the mean axes was localized for the worst displacement condition in Figure 6.3 from each vibration mode, then inputting an upper bound for the mean axes motion: η_1=1.6 e η_2=-0.3. For that, the mean axes definition equations were imposed, that is, $\int_V \vec{p}_d \rho dV\Big|_{RM} = 0$ and $\int_V \vec{p}_e \times \vec{p}_d \rho dV\Big|_{RM} = 0$, where $\vec{p}_e$ is the static position of a point of mass, and $\vec{p}_d$ its displacement.

Doing so, the mean axes is located at $\Delta_{CG} = (0.00, 0.43, 0.02)\,m$ (deformed aircraft CG) in relation to the BRF, and rotated under the eulerian angles $(\Psi, \Theta, \Phi) = (4.98^\circ, 0.22^\circ, 2.49^\circ)$. The CG displacement corresponds to no more than 2% of wing span and the eulerian rotations are such that the transformation matrix $\mathbf{L_{MB}}$ is near to the identity matrix, then justifying the hypothesis for this aircraft.

7 REFERENCES

[1] BISMARCK-NASR, Maher Nasr. **Structural Dynamics in Aeronautical Engineering.** American Institute of Aeronautics and Astronautics, Inc., 1999.
[2] BISPLINGHOFF, R. L., ASHLEY, H., HALFMAN, R. L.. **Aeroelasticity**. Dover Publications, Inc., 1996.
[3] BUTTRILL, C.S., ZEILER, T.A., ARBUCKLE, P.D.. **Nonlinear Simulation of a Flexible Aircraft in Maneuvering Flight**. AIAA Paper 87-2501-CP, AIAA Flight Simulation Technologies Conference, Monterey, CA, agosto, 1987.
[4] CAVIN III, R. K., DUSTO, A. R.. **Hamilton's Principle: Finite Element Methods and Flexible Body Dynamics.** AIAA Journal, Vol. 15, No. 12, 1977.
[5] DOWELL, E. H., CRAWLEY, E. F., CURTISS Jr., H. C., PETERS, D. A., SCANLAN, R. H., SISTO, F.. **A Modern Course in Aeroelasticity, 3rd. Ed.** Kluwer Academic Publishers, 1995.
[6] GOLDSTEIN, H. **Classical Mechanics**. Addison-Wesley Publishing Company, Inc., 1980.
[7] MEIROVITCH, Leonard, TUZCU, Ilhan. **Control of Flexible Aircraft Executing Time-Dependent Maneuvers**. AIAA – Journal of Guidance, Control and Dynamics, Vol. 28, No. 6, November-December 2005.
[8] MEIROVITCH, Leonard, TUZCU, Ilhan. **Integrated Approach to the Dynamics and Control of Maneuvering Flexible Aircraft**. NASA/CR-2003-211748, 2003.
[9] MEIROVITCH, Leonard, TUZCU, Ilhan. **Time Simulations of the Response of Maneuvering Flexible Aircraft**. Journal of Guidance, Control and Dynamics, Vol. 27, No. 5, September-October 2004.
[10] MEIROVITCH, Leonard, TUZCU, Ilhan. **Unified Theory for the Dynamics and Control of Maneuvering Flexible Aircraft**. AIAA Journal, Vol. 42, No. 4, April, 2004.
[11] MEIROVITCH, Leonard. **Fundamentals of Vibrations.** McGraw-Hill, 2001.
[12] MILNE, R. D. **Dynamics of the Deformable Aeroplane**. London: Her Majesty's Stationary Office, 1964.
[13] NELSON, Robert C.. **Flight Stability and Automatic Control, 2nd. Ed**. McGraw-Hill, 1942.
[14] SCHMIDT, D. K., RANEY, D. L.. **Modeling and Simulation of Flexible Flight Vehicles.** Journal of Guidance, Control and Dynamics, Vol. 24, No. 3, 2001.
[15] STEVENS, B. L., LEWIS, F. L.. **Aircraft Control and Simulation, 2nd Edition.** John Wiley & Sons Inc, 2003.
[16] SYNGE, J. L., GRIFFITH, M. A.. **Principles of Mechanics**. McGraw-Hill, 1942.
[17] WASZAK, M. R., BUTTRILL, C. S., SCHMIDT, D. K.. **Modeling and Model Simplification of Aeroelastic Vehicles: An Overview.** NASA Technical Memorandum 107691, 1992.
[18] WASZAK, Martin R., DAVIDSON, John B., SCHIMDT, David K.. **A Simulation Study of the Flight Dynamics of Elastic Aircraft.** Volumes I e II. NASA Contractor Report 4102, 1987.
[19] WASZAK, Martin R.; SCHMIDT, David K.. **Flight Dynamics of Aeroelastic Vehicles.** J. Aircraft, vol. 25, nº. 6, 1998, pág. 563-571.
[20] WU, CHI-HENG. **Flight Dynamics of a Flexible Aircraft**. Doctorate Thesis at the Technische Universität Braunschweig, 1999.

8 RESPONSIBILITY NOTICE

The authors are the only responsible for the printed material included in this paper.